Towards efficient and generic entanglement detection

Jue Xu* and Qi Zhao†
(Dated: September 27, 2022)

Detection of entanglement is an indispensable step for practical quantum computation and communication. In this work, we propose an end-to-end, machine learning assisted entanglement detection protocol. In this protocol, an entanglment witness for a generic entangled state is trained by classical SVM with synthetic data which consist of classical features of quantum state and their labels. In real experiments, classical features of a state, that is expectation values of a set of Pauli measurements, are estimated by sample-efficient methods such as classical shadow.

CONTENTS

I. INTRODUCTION

Entanglement [1] is the key ingredient of quantum computation [2], quantum communication, and quantum cryptography [3]. However, decoherence is inevitable in real-world, which means the interaction between a quantum system and classical environment would greatly affect entanglement quality and diminish quantum advantage. So, for practical purpose, it is essential to benckmark (characterize) entanglement (structures) of certain target states in actual experiments.

The goal of this paper is to find an efficient and generic way to do it. Roughly, our solution is to make use of both machine learning techniques and some recently-developed quantum algorithms. Explicitly, our pipeline starts with a tomographic entanglement witness ansatz which is the linear combination of all possible n-qubit pauli operators. Next, we generate random density matrices with labels for training. Then, we need to evaluate expectation values of each pauli operator, which are features for training a classical SVM. Probably, we can eliminate unimportant features, which means we might not need all pauli operators in our generic witness. Finally, we test and make predictions with brand new samples. In experiments, we make use of classical shadow [4] to estimate classical features of quantum states.

II. PRELIMINARIES

Notation 1. The hats on the matrices such as observables O, entanglement witness W, emphasize that they play the roles of operators (Hermitian matrices). density matrix ρ (omitted) $\{I, X, Y, Z\}$

Notation 2. In the machine learning setting, denote vector (matrix) $\mathbf{x}$, $\mathbf{w}$, $\mathbf{K}$ by boldface font.

Notation 3. If no ambiguity, we omitted the tensor product for readability, that is, $|\psi_A\rangle |\psi_B\rangle \equiv |\psi_A\rangle \otimes |\psi_B\rangle$ and $X^{(1)}Z^{(3)} \equiv \hat{X} \otimes \mathbb{1} \otimes \hat{Z}$.

A. Entanglement structures

Large scale entanglement is the (main) resource of quantum advantages in quantum computation and communication.

Definition 1 (fully separable)**.** An n-qubit pure state $|\psi_f\rangle$ is *fully separable* if and only if it can be written in the tensor product form, i.e., $|\psi_f\rangle = \otimes_i^n |\phi_{A_i}\rangle$. Analoguous to Eq. (1), an n-qubit mixed state ρ_f is fully separable if it can be written as a convex combination of pure full separable states.

Firstly, we consider the simplest entanglement structure: bipartite separable case.

Definition 2 (bipartite separable)**.** Consider a bipartite system AB with the Hilbert space $\mathcal{H}_A \otimes \mathcal{H}_B$, where $\mathcal{H}_A$

* juexu@cs.umd.edu
† zhaoqi@cs.hku.hk

has dimension d_A and $\mathcal{H}_B$ has dimensional d_B, respectively. A pure state $|\psi\rangle$ is *bipartite (bi-)separable* if it is in a tensor product form $|\psi\rangle_{bi} = |\phi\rangle_A \otimes |\phi\rangle_B$, where $\mathcal{P}_2 = \{A, B \equiv \bar{A}\}$ is a bipartition of the qubits in the system. Otherwise, $|\psi\rangle$ is entangled. A mixed state ρ is separable iff it can be written as a convex combination of pure biseparable states with probability distribution $\{p_i\}$

$$\rho_{bi} = \sum_i p_i \, |\psi_i\rangle\langle\psi_i|_{bi} \,, \; \forall p_i > 0, \sum_i p_i = 1 \qquad (1)$$

The set of all bi-separable states is denoted as S_b.

Note that $|\psi_i\rangle$ in Eq. (1) may be bi-separable with respect to different partitions (otherwise genuine multipartite entanglement).

Definition 3 (genuine multipartite entanglement)**.** If a state is not in S_2, it possesses genuine multipartite entanglement (GME).

Note that the state $|\phi\rangle_A$ may be entangled, thus the state $|\psi\rangle$ is not necessarily fully separable. The simple statement "The state is entangled" would still allow that only two of the qubits are entangled while the rest is in a product state. There is another restricted way for the extension to mixed states. A state is $\mathcal{P}_2$-separable, if it is a mixing of pure separable states with a same partition $\mathcal{P}_2$, and we denote the state set as $S_b^{\mathcal{P}_2}$.

For multipartite quantum systems, it is crucial to identify not only the presence of entanglement but also its detailed structure. An identification of the entanglement structure may thus provide us with a hint about where imperfections in the setup may occur, as well as where we can identify groups of subsystems that can still exhibit strong quantum-information processing capabilities.

Given a n-qubit quantum system and its partition into m subsystems, the *entanglement structure* indicates how the subsystems are entangled with each other. In some specific systems, such as distributed quantum computing[] quantum networks[] or atoms in a lattice, the geometric configuration can naturally determine the system partition. Therefore, it is practically interesting to study entanglement structure under partitions.

Definition 4 (fully entangled)**.** An n-qubit quantum state ρ is a *fully entangled*, if it is outside of the separable state set $S_b^{\mathcal{P}_2}$ for any partition, $\rho \notin S_b^{\mathcal{P}_2}, \forall \mathcal{P}_2 = \{A, \bar{A}\}$.

GME is the strongest form of entanglement, that is, all qubits in the system are indeed entangled with each other. The size of the genuinely entangled quantum system becomes a figure of merit for assessing the advancement of quantum devices in the competition among various realizations.

Since $S_b^{\mathcal{P}_2} \subset S_b$, GME is a stronger claim than full entanglement. For a state with full entanglement, it is possible to prepare it by mixing bi-separable states with different bipartitions

Rather than qualitatively determining (bi)separability, there are measures to quantify entanglement.

Definition 5 (concurrence)**.**

Definition 6 (Entanglement intactness, depth)**.** the entanglement intactness of a state ρ to be m, if and only if $\rho \notin S_{m+1}$ and $\rho \in S_m$. When the entanglement intactness is 1, the state possesses genuine multipartite entanglement; and when the intactness is n, the state is fully separable. k-producible. D-dimensional (Schmidt rank) entangled

B. Entanglement detection

Many methods [5] have been developed to determine whether a state is bi-separable.

Problem 1 (separability)**.** given (input) an **unknown** state, to determine (output) (bi-)separability.

in theoretic CS language

Problem 2 (Weak membership problem for separability)**.** Given a density matrix ρ_{AB} with the promise that either (i) $\rho_{AB} \in S_{bi}$ or (ii) $\|\rho_{AB} - S\| \geq \epsilon$, decide which is the case.

Theorem 1 (PPT criterion)**.** *If a state is bipartite separable, then it must have positive partial transpose (PPT), that is, the partially transposed (PT) density matrix $\rho_{AB}^{\mathsf{T}_A}$ is positive, semidefinite [6]. Equivalently, if the smallest eigenvalue of partial transpose $\rho_{AB}^{\mathsf{T}_A}$ is negative, then the state is (fully?) entangled. Note that PPT is a necessary and sufficient condition for separability when $d_A d_B \leq 6$ [7].*

PPT criterion Classically, the hardness of determining the bipartite separability. Another widely used one is the k-symmetric extension hierarchy [8], which is presently one of the most powerful criteria, but hard to compute in practice due to its exponentially growing complexity with k.[??] In order to apply the PPT criterion (the minimum eigenvalue of the partial-transposed density matrix), the full density matrix must be available. However, quantum state tomography requires an exponential number of measurements.

However, up to now, no general solution for the separability problem is known. Similar to the PPT condition, the p_3-PPT condition applies to mixed states and is completely independent of the state in question. This is a key distinction from entanglement witnesses, which can be more powerful, but which **usually require detailed prior information about the state**. From this data set, the PT-moments p_n can be estimated without having to reconstruct the density matrix ρ_{AB}, and with a significantly smaller number of experimental runs M than required for full quantum state tomography.

Theorem 2 ([9])**.** *Weak membership problem for separability is NP-Hard for $\epsilon = 1/\operatorname{poly}(D)$ (with respect to Euclidean norm and trace norm). [10] [11] quasipolynomial-time algorithm ($\|\cdot\|_2$ and $\|\cdot\|_{LOCC}$) [12]*

However, we do not know approximately correct complexity? quantum complexity? machine learning (data)? for entanglement () problem? multipartite?

Problem 3 (Entanglement detection)**.** Different from separability problem, we assume prior knowledge of the target state $|\psi\rangle$

- **Input**: a (unknown, experiment) state ρ in the 'vicinity' of $|\psi\rangle$ (undergo noise channels: white noise, bit/phase-flip error, random local unitary);
- **Output**: whether ρ has 'useful' entanglement or not (GME, full entanglement, $S_b^{\mathcal{P}}$, intactness, depth ...)

difficulty: multi(n)-partite, high-dimensional (qudit) [13], pure/mixed state, with/out prior knowledge, universal?, non-stabilizer [5], certain partition

Bell inequalities as the oldest tool to detect entanglement [14]. Originally, Bell inequalities were designed to rule out local hidden variable (LHV) models.

Definition 7 (CHSH inequality)**.** CHSH inequality (game) ...; $\hat{\mathbf{p}} = (\mathbb{1}, ab, ab', a'b, a'b')$

$$a = Z, a' = X, b = (X - Z)/\sqrt{2}, b = (X + Z)/\sqrt{2}, \quad (2)$$

features as the input. CHSH operator $W_{\text{CHSH}} := \hat{\mathbf{p}} \cdot \mathbf{w}_{\text{CHSH}}$ with $\mathbf{w}_{\text{CHSH}} = \{\pm 2, 1, -1, 1, 1\}$

However, even for two-qubit systems there exist entangled states which do not violate any Bell inequality. [15] For example, the maximally-entangled Bell state can maximally violate the CHSH inequality, but this state mixed with certain extent white noise (2/3) don't violate the CHSH inequality despite it is still entangled.

does not require any a priori knowledge about the quantum state. For $\text{Tr}(\rho_A^m)$, an important application of multivariate trace estimation [16] is to entanglement spectroscopy [17] [18] [19] - deducing the full set of eigenvalues of ρ_A. The smallest eigenvalue of diagnoses whether ψ_{AB} is separable or entangled [20]. The well-known identity (related to the replica trick originating in spin glass theory)

$$\text{Tr}(U^\pi(\rho_1 \otimes \cdots \otimes \rho_m)) = \text{Tr}(\rho_1 \cdots \rho_m) \quad (3)$$

where the RHS is the multivariate trace and U^π is a unitary representation of the cyclic shift permutation. Direct entanglement detections, can be employed as subroutines in quantum computation and realized by quantum circuits because it is naturally quantum data.

estimate the spectrum by quantum constant depth circuits, but this method only works for bipartite. (can we estimate concurrence by quantum circuit? quantum kernel SVM?) solve the quantum problem by quantum, without full tomography. unknown how to generalize to multipartite.

1. *Entanglement witness based on fidelity*

While various methods for constructing an entanglement witness exist, one of the most common is based on the fidelity of a state to a pure entangled state. Another approach for detecting multipartite entanglement is using entanglement witnesses. Different Bell inequalities can be regarded as entanglement witness for different types of entanglement in a multi-party entangled state. These witnesses can be quite useful to detect entanglement in the vicinity of graph states.

see Fig. 1 for relations. entanglement detection [21].

Definition 8 (entanglement witness)**.** Given a speific entangled state $|\psi\rangle_{\text{tar}}$, its *entanglement witness* W is an obseverable such that

$$\text{Tr}(W\rho_{bi}) \geq 0 \text{ and } \text{Tr}(W|\psi_{\text{tar}}\rangle\langle\psi_{\text{tar}}|) < 0 \quad (4)$$

In general, an entanglement witness is an observable which has a positive expectation value on all separable states, hence a negative mean value implys the presence of entanglement.

In a typical experiment one aims to prepare a pure state, $|\psi\rangle$, and would like to detect it as true multipartite entangled. While the preparation is never perfect, it is still expected that the prepared mixed state is in the proximity of $|\psi\rangle$. The usual way to construct entanglement witnesses using the knowledge of this state is

$$W_\psi = \alpha\mathbb{1} - |\psi\rangle\langle\psi| \quad (5)$$

where α is the smallest constant such that for every product state $\text{Tr}(\rho W) \geq 0$. This kind of witness is projector-based witness [22]. However, it is generally difficult to evaluate the quantity $\text{Tr}(\rho_{\text{pre}}|\psi_{\text{tar}}\rangle\langle\psi_{\text{tar}}|)$ by the direct projection, because the target state is an entangled state. In order to measure the witness in an experiment, it is supposed be decomposed into a sum of locally measurable operators. The number of local measurements in these decompositions seems to increase exponentially with the number of qubits.[??] local measurements [23] stabilizer [5] graph state [24]

Proposition 1 (Section 6.3 of [25])**.** *A state ρ is separable iff $\forall W, \text{Tr}[\rho W] \geq 0$. Corollary, a state ρ is entangled iff $\exists W, \text{Tr}[\rho W] < 0$. There is no entanglement witness that detects all entangled states.*

It is natural to ask how nonlinear entanglement witness [26] and the kernel method (nonlinear boundary) in machine learning can be applied.

2. *Beyond fidelity and stabilizer witness (robustness)*

coherent noise [27]. local unitary/rotation Unconscious phase accumulation Rotation on the first control qubit

$$|\psi(\phi, \theta)\rangle = \cos\theta|000\rangle + e^{i\phi}\sin\theta|111\rangle \quad (6)$$

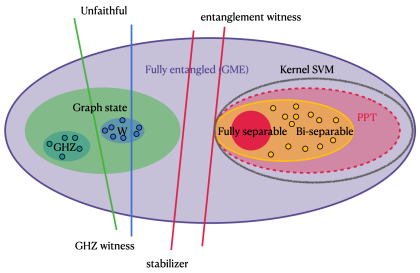

FIG. 1: (a) entanglement witness, PPT criterion, SVM (kernel)?. convex hull... The witness is depicted by the line in state space $\mathrm{Tr}(\rho W) = 0$

the authors coined the term faithful. Weilenmann et. al [28] proposed the idea of unfaithful states which systematically analyze entangled state with noise cannot be detected by fidelity witness. faithful states are useful for quantum teleportation. This shows that fidelity-based entanglement witnesses detect entanglement that is useful. [29] the faithfulness of a twoqubit state, allowing for a physical interpretation of unfaithful two-qubit states as exactly those entangled states that are not useful for teleportation. [30] [31]

Definition 9 (unfaithful state)**.** informally, unfaithful state are entangled states but cannot be detected by fidelity witness. a state ρ_{AB} is faithful if and only if there are local unitary transformations U_A and U_B such that

$$\langle \phi^+ | U_A \otimes U_B \rho_{AB} U_A^\dagger \otimes U_B^\dagger | \phi^+ \rangle > \frac{1}{d} \tag{7}$$

They found that for $d \geq 3$ that almost all states in the Hilbert space are unfaithful. For $d > 5$, the authors find that all states they generated are entangled but at the same time unfaithful, regardless of what metric is used to sample them. Although there are nonlinear witnesses which also can detect entanglement in unfaithful states, they usually require more measurements []. Moreover, they can only be applied to bipartite systems, which means they cannot be generalized to detect genuine entanglement in multipartite states. Detecting Entanglement in Unfaithful States [32].

For non-stabilizer case, [33] [34] C is hard to compute? non-stabilizer state? SWAP? p_{noise} indicates the robustness of the algorithm (witness). the largest noise tolerance p_{limit} just related to the **chromatic number** of the graph (k local measurements) [24].(**??**) find optimal (robustness) entanglement witness by classical machine learning (quantum circuit?) tradeoff between (white noise) tolerance (robustness) and efficiency (number of measurements).

III. END-TO-END ENTANGLEMENT DETECTION PROTOCOL

In this paper, we focus on the entanglement structure dectection for graph states. with training data

Problem 4 (Learning an entanglement witness with training data)**.** Different from Entanglement detection, we assume training data

- **Input**: specific entanglement structures y and corresponding synthetic data (density matrices ρ) with labels y
- **Output**: find the classifier $\mathbf{w}$ with high accuracy and minimal features $\mathbf{x} :=$

The idea is to feed the classifier by a large amount of sampled trial states as well as their corresponding class labels.

A. Training a generic witness via SVM

classical machine learning (SVM, NN) with classical shadow [35]??: classify phase, predict ground state, entanglement? The quantum extension of this problem (classficiation/pattern recognition) is to replace the data points $\mathbf{x}_i$ with density matrices of quantum states ρ_i. Specifically, a quantum state classifier outputs a "label" associated with the state, for example, entangled or "unentangled". In actual experiments, we don't know entries of a density matrix. Instead, we need measurements or classical shadow as features of machine learning algorithms.

Lu et. al [36] separability classifier by classical neural network: input: sythetic random density matrices; output: a universal classifier for bipartite separable. (feature: synthetic density matrix with noise flatten as a real vector $\mathbf{x} \in \mathbb{R}^{d_A^2 d_B^2 - 1}$). For the same purpose, Ma and Yung [15] generalize Bell inequlaity and tomographic witness by neural network. a linear Bell-like predictor by generalizing the CHSH operator $W_{\text{ml}} := \mathbf{P} \cdot \mathbf{w}_{\text{ml}}$ in Eq. (2) where the coefficients (or weights) $\mathbf{w}$ are determined by machine learning. tomographic ansatz better performance. training a universal classifier for multiqubit, high-dimensional system is hard (boundary). it is difficult to generate general GME states or label general states. Tomography is necessary for universal entanglement detection with single-copy observables (nonadaptive schemes) [37]

classical SVM: [34] This method the ability to obtain witnesses that require only local measurements even when the target state is a **non-stabilizer state** W state (normally need nonlocal measurements). feature: $\mathbf{x}_{\vec{k}}$ expectation of Pauli strings. the training of an SVM is convex; if a solution exists for the given target state and ansatz, the optimal SVM will be found. this SVM formalism allows for the programmatic removal of features,

i.e., reducing the number of experimental measurements, in exchange for a lower tolerance to white noise, in a manner similar to [??]. SVM, (universal), 4 qubit [38]

	# observables	weights	input state
fidelity witness	few local	fixed	known
Bell (CHSH) inequality	constant	fixed	unknown
tomographic classifier [15]	$4^n - 1$	trained	unknown
SVM witness	??	trained	partial

TABLE I: ansatz

an ansatz for entanglement witness

$$W_{\text{ansatz}} := \sum_{\mathbf{p}\in\{I,X,Y,Z\}^n} w_{\mathbf{p}} \bigotimes_i^n \mathbf{p}_i \tag{8}$$

c.f. quantum state tomography (Stokes parameters) **??**. An SVM allows for the construction of a hyperplane $\langle W\rangle = \sum_k w_k \mathbf{x}_k$ that clearly delineates between separable states and the target entangled state (bipartite and **tripartite qubit and qudit**); this hyperplane is a **weighted sum of observables ('features') whose coefficients are optimized during the training of the SVM**.

We focus on kernel methods, as they not only provide provable guarantees, but are also very flexible in the functions they can learn. For example, recent advancements in theoretical machine learning show that training neural networks with large hidden layers is equivalent to training an ML model with a particular kernel, known as the neural tangent kernel [39].

Algorithm III.1: train witness with SVM

input : training data with labels
output: classifier $\mathbf{w}_{\text{ml}}$

for $i = 1, 2, \ldots, m$ **do**
  kernel estimation `// classical kernel`
  SVM `// SVM`
  return parameters $\mathbf{w}_{\text{ml}}$
`// call Algorithm. III.2`
return $\mathbf{w}\cdot\vec{\sigma} < 0$: separable `/* predict */`

1. *Data preparation and state generation*

multi-partite entangled state: generate synthetic (engineered) data from (random graph?). separable state from randomly ...

QuTiP library [40]; quantum circuit [41]

entangled states generation: Bell, GHZ, W state, graph (cluster) state

separable states generation

- 2-qubit: bipartite Eq. (6)
- Training data for $\rho_b^{(1,2,3)}$ generated by sampling over the Hilbert-Schmidt-distributed space of single-qubit and bi-qubit density matrices. As for the entangled state, we again use the Werner state to generate the training data for that class of states.

$$\rho_{A|B|C},\ \rho_{A|BC},\ \rho_{AB|C},\ \rho_{B|AC} \tag{9}$$

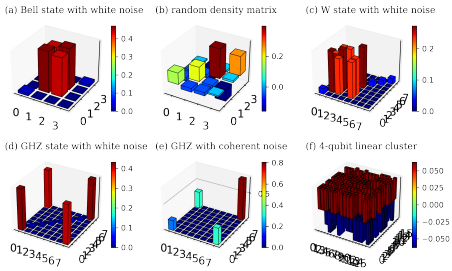

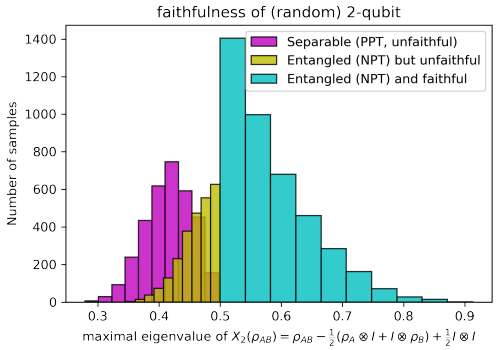

FIG. 2: data praparation: random states (a) three-qubit W state, (b) GHZ state with white noise (c) (d) (e) PPT

B. Sample-efficient trace estimation methods

To make use of classical machine learning method, we need the classical **features** of quantum states. We cannot directly process quantum data (raw data). In our pipeline, we focus on classical shadow.

classical shadow [4]: estimate entanglment witness (fixed but unknown target state, e.g., tripartite GHZ) **Classical shadows (Clifford measurements) of logarithmic size allow for checking a large number of potential entanglement witnesses simultaneously**. Directly measuring M different entanglement witnesses requires a number of quantum measurements that scales (at least) linearly in M. In contrast, classical shadows get by with $\log(M)$-many measurements only. classical shadows are based on random Clifford measurements and do not depend on the structure of the concrete witness in question. In contrast, direct estimation crucially depends on the concrete witness in question and may be considerably more difficult to implement.

The brute force approach is to fully characterize a system by performing quantum state tomography and calculating separability measures from the recovered den-

sity matrix. Intuitively, a general tomography [42] that extract (recover) all information of a state requires exponential copies (samples/measurements).

Problem 5 (quantum state tomography)**.** Informally, quantum state tomography refers to the task of estimating complete description (density matrix) of an unknown N-dimensional quantum mixed state ρ within some error, given the ability to prepare and measure m copies $\rho^{\otimes m}$.

However, tomography is experimentally and computationally demanding; for a state consisting of n particles, with each residing in a d-dimensional Hilbert space, we would have to perform $M = \mathcal{O}(d^{2n})$ measurements.

Theorem 3 (lower bound of quantum state tomography?[43])**.** *Known fundamental lower bounds [66, 73] state that classical shadows of exponential size (at least) $T = \Omega(2^n/\epsilon^2)$ are required to ϵ-approximate ρ in trace distance. [35]*

In quantum mechanics, interesting properties are often linear functions of the underlying density matrix ρ. For example, the fidelity with a pure target state, entanglement witnesses fit this framework.

Problem 6 (trace estimation)**.** related problems defined as follows

- **Input**: Given an observable (Hermitian) O and (copies of) a mixed state ρ or several states $(\rho', \dots, \rho_m)$,
- **Output**: with error ϵ measured by trace distance (fidelity...), to estimate linear functions (mostly): the expectation value $\langle O\rangle = \mathrm{Tr}(O\rho)$, entanglement witness, tomography; nonlinear functions: entropy; multivariate functions: $\mathrm{Tr}(\rho_1 \cdots \rho_m)$, quantum kernel $\mathrm{Tr}(\rho\rho')$, quadratic $\mathrm{Tr}(O\rho_i \otimes \rho_j)$, fidelity $F(\rho, \rho')$, distance??;

Nevertheless, we usually only need specific properties of a target state rather than full classical descriptions about the state. This enables the possibility to shadow tomography.

Problem 7 (shadow tomography)**.** *shadow tomography*

- **Input**: an **unknown** N-dimensional mixed state ρ, M known 2-outcome measurements $E_1, \dots, E_M$
- **Output**: estimate $\mathbb{P}[E_i \text{ accept } \rho]$ to within additive error ϵ, $\forall i \in [M]$, with $\geq 2/3$ success probability.

Theorem 4 (bounds of shadow tomography [44])**.** *It is possible to do shadow tomography using $\tilde{\mathcal{O}}(\frac{\log^4 M \cdot \log N}{\epsilon^4})$ copies. [no construction algorithm?] sample complexity lower bound $\Omega(\log(M) \cdot \epsilon^{-2})$,*

Remark 1 (compare shadow tomography with classical shadow [4])**.** While very efficient in terms of samples, Aaronson's procedure is very demanding in terms of quantum hardware - a concrete implementation of the proposed protocol requires **exponentially long quantum circuits** that act collectively on all the copies of the unknown state stored in a quantum memory.

1. *Classical shadow and derandomized version*

Inspired by Aaronson's shadow tomography [44], Huang et. al [4] introduce classical shadow. A classical shadow is a succinct classical description of a quantum state, which can be extracted by performing reasonably simple single-copy measurements on a reasonably small number of copies of the state. The classical shadow attempts to approximate this expectation value by an empirical average over T independent samples, much like Monte Carlo sampling approximates an integral.

Definition 10 (classical shadow)**.** Given a quantum state ρ, its classical shadow (snapshots) ρ_{cs} is

$$\rho_{cs} := \mathcal{M}^{-1}\left(U^\dagger \left|\hat{b}\right\rangle\!\left\langle\hat{b}\right| U\right) \tag{10}$$

where $|b\rangle$ is ... $U\rho U^\dagger$ such that we can predict the linear function with classical shadows

$$o_i = \mathrm{Tr}(O_i\rho_{cs}) \text{ obeys } \mathbb{E}[o] = \mathrm{Tr}(O_i\rho) \tag{11}$$

The classical shadow size required to accurately approximate all reduced r-body density matrices scales exponentially in subsystem size r, but is independent of the total number of qubits n.

Algorithm III.2: Estimate features by classical shadow

input : samples of ρ and $W_{\mathrm{ml}} := \mathbf{P} \cdot \mathbf{w}$
output: estimation of $\mathrm{Tr}(W_{\mathrm{ml}}\rho)$

for $i = 1, 2, \dots, N$ **do**
  $\rho \mapsto U\rho U^\dagger$ `// apply a random unitary to rotate the state`
  $\mapsto |b\rangle$... `// perform a computational-basis measurement`
  $\rho_{cs} = \mathcal{M}^{-1}(U^\dagger |b\rangle\langle b| U)$ `// measurement outcome` $|b\rangle \in \{0,1\}^n$, $\mathcal{M}$ `quantum channel`
return $S(\rho, N) = \left\{\rho_{cs_1} = \mathcal{M}^{-1}\left(U_1^\dagger |b_1\rangle\langle b_1| U_1\right), \dots, \rho_{cs_N}\right\}$ `// call this array the classical shadow of` ρ
`/* estimate features */`
return estimation of $\mathrm{Tr}(W\rho)$

A classical shadow is created by repeatedly performing a simple procedure: Apply a unitary transformation $\rho \mapsto U\rho U^\dagger$, and then measure all the qubits in the computational basis. The number of times this procedure is repeated is called the size of the classical shadow. The transformation U is randomly selected from an ensemble of unitaries, and different ensembles lead to different versions of the procedure that have characteristic strengths and weaknesses. Classical shadows with size of order $\log(M)$ suffice to predict M target functions $\{O_1, \dots, O_M\}$.

Theorem 5 (Pauli/Clifford measurements)**.** *Any procedure based ona fixed set of single-copy local measurements that can predict, with additive error ϵ, M arbitrary k-local linear function $\mathrm{Tr}(O_i\rho)$, requires at least*

(lower bound) $\Omega(\log(M)3^k/\epsilon^2)$ *copies of the state* ρ. $\Omega(\log(M)\max_i \mathrm{Tr}(O_i^2)/\epsilon^2)$

Derandomization can and should be viewed as a refinement of the original classical shadows idea. [45] [19]

2. *Estimate expectation by (classical/quantum) machine learning*

[35] $\sigma_T(\rho(x_l))$ is the classical shadow representation of $\rho(x_l)$, a $2^n \times 2^n$ matrix that reproduces $\rho(x_l)$ in expectation over random Pauli measurements.

$$\{x_l \to \sigma_T(\rho(x_l))\}_{l=1}^N \tag{12}$$

Definition 11 (shadow kernel)**.** given two density matrices (quantum states) ρ and ρ', *shadow kernel* [4] is

$$k_{\text{shadow}}(S_T(\rho), S'_T(\rho')) := \exp\left(\frac{\tau}{T^2}\sum_{t,t'=1}^{T}\exp\left(\frac{\gamma}{n}\sum_{i=1}^{n}\mathrm{Tr}\left(\sigma_i^{(t)}\sigma_i^{(t')}\right)\right)\right) \tag{13}$$

where $S_T(\rho)$ is the classical shadow representation of ρ. The computation time for the inner product is $\mathcal{O}(nT^2)$, linear in the system size n and quadratic in T, the number of copies of each quantum state which are measured to construct the classical shadow.

though, that while there is no large advantage in query complexity, a substantial quantum advantage in computational complexity is possible.

The quantum ML algorithm accesses the quantum channel $\mathcal{E}_\rho$ multiple times to obtain multiple copies of the underlying quantum state ρ. Each access to $\mathcal{E}_\rho$ allows us to obtain one copy of ρ. Then, the quantum ML algorithm performs a sequence of measurements on the copies of ρ to accurately predict $\mathrm{Tr}(P_x\rho), \forall x \in \{I, X, Y, Z\}^n$.

Theorem 6 ([46])**.** *For M Pauli opertors, there is a (quantum) procedure estimate every expectation value $\mathrm{Tr}(P_x\rho), \forall i = 1, \ldots, M$ within error ϵ under probability at least $1-\delta$ by performing POVM measurements on $\mathcal{O}(\log(M/\delta)\epsilon^{-4})$ copies of the unknown quantum state ρ. ($M = 4^n$ implies linear copy for full tomography???) We rigorously show that, for any quantum process $\mathcal{E}$, observables O, and distribution $\mathcal{D}$, and for any quantum ML model, one can always design a classical ML model achieving a similar average prediction error such that N_C (number of experiments?) is larger than N_Q by at worst a small polynomial factor.*

In contrast, for achieving accurate prediction on all inputs, we prove that ***exponential quantum advantage is possible****. For example, to predict expectations of all* ***Pauli observables*** *(entanglement witness??) in an n-qubit system ρ, classical ML models require $2^{\Omega(n)}$ copies of ρ , but we present a quantum ML model using only $\mathcal{O}(n)$ copies.*

[4] [46] [47] [44]
generative neural network [48]

	circuits / sample complexity
shadow tomography	exp circuit? Theorem 4
classical shadow	
derandomized CS	better performance
quantum circuit	**??** (c-depth?) ?
quantum/classical ML	Q. advantage Theorem 6

TABLE II: complexity (measures) of different trace estimation methods

IV. NUMERICAL SIMULATION

A. Classification accuracy and comparison

1. *Hyperparameters and settings*

We consider a set of different regularization parameters,..

The goal of RFE is to eliminate non-essential features by recursively considering smaller and smaller subsets of the original features using a greedy algorithm. Initially, RFE takes the SVM we trained and ranks the coefficients by their magnitudes, with the lowest one pruned away; then the model is trained again with the remaining features.

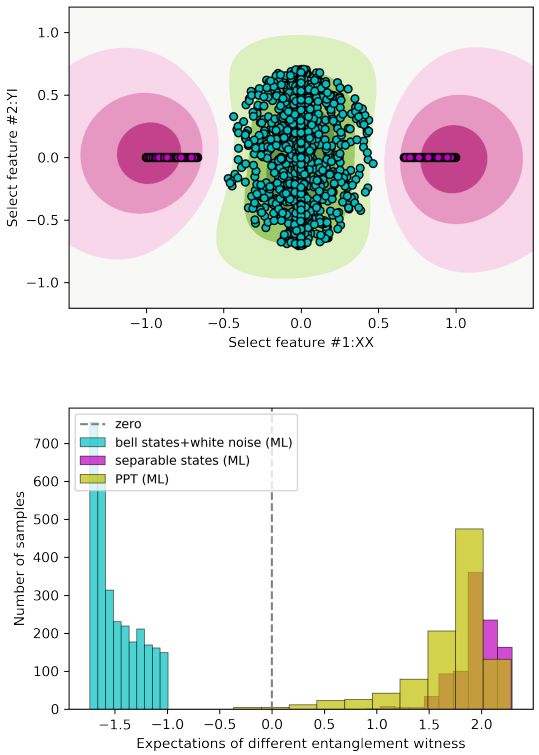

FIG. 3: (a) two-dimensional embedding: feature space, recursive feature elimination; (b) feature ranking

FIG. 4: accuracies (variance) VS different data sizes

FIG. 5: number of features VS number of qubits (n). feature elimination

2. *Results, feature elimination*

performance of different methods: for any state ρ_s with only bipartite entanglement, $\mathrm{Tr}(O\rho_s) \leq 0.5$, while for any state ρ_s with at most W-type entanglement, $\mathrm{Tr}(O\rho_s) \leq 0.75$. Therefore verifying that $\mathrm{Tr}(O\rho) \geq 0.5$ certifies that ρ has tripartite entanglement, while $\mathrm{Tr}(O\rho) > 0.75$ certifies that ρ has GHZ-type entanglement. [49]

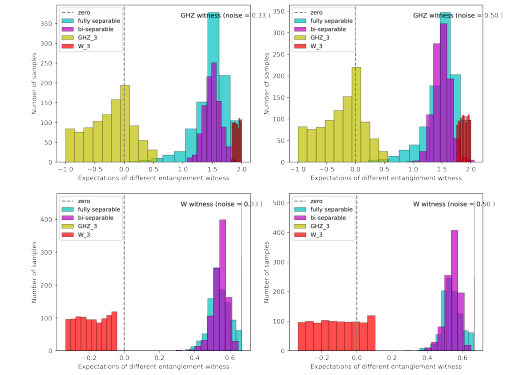

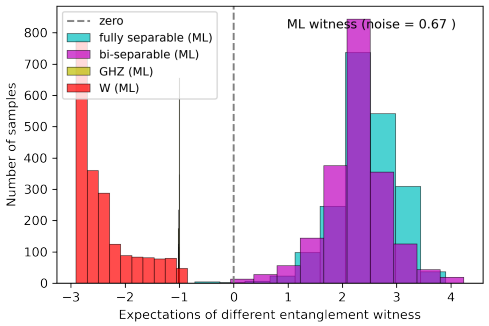

FIG. 6: (a) compare different methods: Bell inequality, witness, ML ansatz; different white noise limit, unfaithful state; (b) ML witness for unfaithful (large white noise), non-stabilizer (W) state

V. EXPERIMENTS

future: experimental (photonic) implementation with a few qubits (generation, verification) [50]. fully entangled graph state (ring of 16 qubits) IBM by measuring negativity [51] optical lattice [52] (homogeneous, restricted measurement, different noise channels; detect GME, full entanglement). classical shadow experiments [53] [19]

VI. CONCLUSION AND DISCUSSION

ACKNOWLEDGMENTS

[1] R. Horodecki, P. Horodecki, M. Horodecki, and K. Horodecki, Rev. Mod. Phys. **81**, 865 (2009), arXiv:quant-ph/0702225.
[2] H. J. Briegel, D. E. Browne, W. Dür, R. Raussendorf, and M. V. den Nest, Nature Phys **5**, 19 (2009), arXiv:0910.1116.
[3] F. Xu, X. Ma, Q. Zhang, H.-K. Lo, and J.-W. Pan, Rev. Mod. Phys. **92**, 025002 (2020), arXiv:1903.09051.
[4] H.-Y. Huang, R. Kueng, and J. Preskill, Nat. Phys. **16**, 1050 (2020), arXiv:2002.08953 [quant-ph].

[5] G. Tóth and O. Gühne, Phys. Rev. A **72**, 022340 (2005).
[6] A. Peres, Phys. Rev. Lett. **77**, 1413 (1996), arXiv:quant-ph/9604005.
[7] M. Horodecki, P. Horodecki, and R. Horodecki, Physics Letters A **223**, 1 (1996), arXiv:quant-ph/9605038.
[8] M. Navascues, M. Owari, and M. B. Plenio, Phys. Rev. A **80**, 052306 (2009), arXiv:0906.2731 [quant-ph].
[9] L. Gurvits, Classical deterministic complexity of Edmonds' problem and Quantum Entanglement (2003), arXiv:quant-ph/0303055.
[10] L. M. Ioannou, Quantum Inf. Comput. **7**, 335 (2007), arXiv:quant-ph/0603199.
[11] A. C. Doherty, P. A. Parrilo, and F. M. Spedalieri, Phys. Rev. A **69**, 022308 (2004), arXiv:quant-ph/0308032.
[12] F. G. S. L. Brandao, M. Christandl, and J. Yard, A quasipolynomial-time algorithm for the quantum separability problem (2011), arXiv:1011.2751 [quant-ph].
[13] S. Sciara, C. Reimer, M. Kues, P. Roztocki, A. Cino, D. J. Moss, L. Caspani, W. J. Munro, and R. Morandotti, Phys. Rev. Lett. **122**, 120501 (2019).
[14] B. M. Terhal, Physics Letters A **271**, 319 (2000), arXiv:quant-ph/9911057.
[15] Y.-C. Ma and M.-H. Yung, npj Quantum Inf **4**, 34 (2018), arXiv:1705.00813 [quant-ph].
[16] Y. Quek, M. M. Wilde, and E. Kaur, Multivariate trace estimation in constant quantum depth (2022), arXiv:2206.15405 [hep-th, physics:quant-ph].
[17] A. K. Ekert, C. M. Alves, D. K. L. Oi, M. Horodecki, P. Horodecki, and L. C. Kwek, Phys. Rev. Lett. **88**, 217901 (2002), arXiv:quant-ph/0203016.
[18] S. Johri, D. S. Steiger, and M. Troyer, Phys. Rev. B **96**, 195136 (2017), arXiv:1707.07658.
[19] A. Elben, R. Kueng, H.-Y. Huang, R. van Bijnen, C. Kokail, M. Dalmonte, P. Calabrese, B. Kraus, J. Preskill, P. Zoller, and B. Vermersch, Phys. Rev. Lett. **125**, 200501 (2020), arXiv:2007.06305 [cond-mat, physics:quant-ph].
[20] P. Horodecki and A. Ekert, Phys. Rev. Lett. **89**, 127902 (2002), arXiv:quant-ph/0111064.
[21] O. Gühne and G. Toth, Physics Reports **474**, 1 (2009), arXiv:0811.2803 [cond-mat, physics:physics, physics:quant-ph].
[22] M. Bourennane, M. Eibl, C. Kurtsiefer, S. Gaertner, H. Weinfurter, O. Guehne, P. Hyllus, D. Bruss, M. Lewenstein, and A. Sanpera, Phys. Rev. Lett. **92**, 087902 (2004), arXiv:quant-ph/0309043.
[23] G. Toth and O. Guehne, Phys. Rev. Lett. **94**, 060501 (2005), arXiv:quant-ph/0405165.
[24] Y. Zhou, Q. Zhao, X. Yuan, and X. Ma, npj Quantum Inf **5**, 83 (2019).
[25] T. Heinosaari and M. Ziman, *The Mathematical Language of Quantum Theory: From Uncertainty to Entanglement*, 1st ed. (Cambridge University Press, 2011).
[26] O. Gühne and N. Lütkenhaus, Phys. Rev. Lett. **96**, 170502 (2006).
[27] Y. Zhou, Phys. Rev. A **101**, 012301 (2020), arXiv:1907.11495 [quant-ph].
[28] M. Weilenmann, B. Dive, D. Trillo, E. A. Aguilar, and M. Navascués, Phys. Rev. Lett. **124**, 200502 (2020), arXiv:1912.10056 [quant-ph].
[29] O. Gühne, Y. Mao, and X.-D. Yu, Phys. Rev. Lett. **126**, 140503 (2021), arXiv:2008.05961 [quant-ph].
[30] G. Riccardi, D. E. Jones, X.-D. Yu, O. Gühne, and B. T. Kirby, Exploring the relationship between the faithfulness and entanglement of two qubits (2021), arXiv:2102.10121 [quant-ph].
[31] X.-M. Hu, W.-B. Xing, Y. Guo, M. Weilenmann, E. A. Aguilar, X. Gao, B.-H. Liu, Y.-F. Huang, C.-F. Li, G.-C. Guo, Z. Wang, and M. Navascués, Phys. Rev. Lett. **127**, 220501 (2021).
[32] Y. Zhan and H.-K. Lo, Detecting Entanglement in Unfaithful States (2021), arXiv:2010.06054 [quant-ph].
[33] Y. Zhang, Y. Tang, Y. Zhou, and X. Ma, Phys. Rev. A **103**, 052426 (2021), arXiv:2012.07606 [quant-ph].
[34] E. Y. Zhu, L. T. H. Wu, O. Levi, and L. Qian, Machine Learning-Derived Entanglement Witnesses (2021), arXiv:2107.02301 [quant-ph].
[35] H.-Y. Huang, R. Kueng, G. Torlai, V. V. Albert, and J. Preskill, Provably efficient machine learning for quantum many-body problems (2021), arXiv:2106.12627 [quant-ph].
[36] S. Lu, S. Huang, K. Li, J. Li, J. Chen, D. Lu, Z. Ji, Y. Shen, D. Zhou, and B. Zeng, Phys. Rev. A **98**, 012315 (2018), arXiv:1705.01523 [quant-ph].
[37] D. Lu, T. Xin, N. Yu, Z. Ji, J. Chen, G. Long, J. Baugh, X. Peng, B. Zeng, and R. Laflamme, Phys. Rev. Lett. **116**, 230501 (2016), arXiv:1511.00581 [quant-ph].
[38] S. V. Vintskevich, N. Bao, A. Nomerotski, P. Stankus, and D. A. Grigoriev, Classification of four-qubit entangled states via Machine Learning (2022), arXiv:2205.11512 [quant-ph].
[39] A. Jacot, F. Gabriel, and C. Hongler, Neural Tangent Kernel: Convergence and Generalization in Neural Networks (2020), arXiv:1806.07572 [cs, math, stat].
[40] J. R. Johansson, P. D. Nation, and F. Nori, Computer Physics Communications **184**, 1234 (2013), arXiv:1110.0573.
[41] B. Li, S. Ahmed, S. Saraogi, N. Lambert, F. Nori, A. Pitchford, and N. Shammah, Quantum **6**, 630 (2022), arXiv:2105.09902 [quant-ph].
[42] J. Altepeter, E. Jeffrey, and P. Kwiat, in *Advances In Atomic, Molecular, and Optical Physics*, Vol. 52 (Elsevier, 2005) pp. 105–159.
[43] J. Haah, A. W. Harrow, Z. Ji, X. Wu, and N. Yu, IEEE Trans. Inform. Theory , 1 (2017).
[44] S. Aaronson, in *Proc. 50th Annu. ACM SIGACT Symp. Theory Comput.*, STOC 2018 (Association for Computing Machinery, New York, NY, USA, 2018) pp. 325–338, arXiv:1711.01053.
[45] H.-Y. Huang, R. Kueng, and J. Preskill, Phys. Rev. Lett. **127**, 030503 (2021), arXiv:2103.07510 [quant-ph].
[46] H.-Y. Huang, R. Kueng, and J. Preskill, Phys. Rev. Lett. **126**, 190505 (2021), arXiv:2101.02464 [quant-ph].
[47] H.-Y. Huang, M. Broughton, M. Mohseni, R. Babbush, S. Boixo, H. Neven, and J. R. McClean, Nat Commun **12**, 2631 (2021), arXiv:2011.01938 [quant-ph].
[48] Y. Zhu, Y.-D. Wu, G. Bai, D.-S. Wang, Y. Wang, and G. Chiribella, Flexible learning of quantum states with generative query neural networks (2022), arXiv:2202.06804 [quant-ph].
[49] A. Acin, D. Bruss, M. Lewenstein, and A. Sanpera, Phys. Rev. Lett. **87**, 040401 (2001), arXiv:quant-ph/0103025.
[50] H. Lu, Q. Zhao, Z.-D. Li, X.-F. Yin, X. Yuan, J.-C. Hung, L.-K. Chen, L. Li, N.-L. Liu, C.-Z. Peng, Y.-C. Liang, X. Ma, Y.-A. Chen, and J.-W. Pan, Phys. Rev. X **8**, 021072 (2018).
[51] Y. Wang, Y. Li, Z.-q. Yin, and B. Zeng, npj Quantum Inf **4**, 46 (2018), arXiv:1801.03782.

[52] Y. Zhou, B. Xiao, M.-D. Li, Q. Zhao, Z.-S. Yuan, X. Ma, and J.-W. Pan, npj Quantum Inf **8**, 1 (2022).
[53] T. Zhang, J. Sun, X.-X. Fang, X.-M. Zhang, X. Yuan, and H. Lu, Experimental quantum state measurement with classical shadows (2021), arXiv:2106.10190 [physics, physics:quant-ph].
[54] C. Bădescu, R. O'Donnell, and J. Wright, Quantum state certification (2017), arXiv:1708.06002 [quant-ph].
[55] M. Hein, W. Dür, J. Eisert, R. Raussendorf, M. V. den Nest, and H.-J. Briegel, Entanglement in Graph States and its Applications (2006), arXiv:quant-ph/0602096.
[56] L. Bai, L. Rossi, A. Torsello, and E. R. Hancock, Pattern Recognition **48**, 344 (2015).
[57] V. Havlicek, A. D. Córcoles, K. Temme, A. W. Harrow, A. Kandala, J. M. Chow, and J. M. Gambetta, Nature **567**, 209 (2019), arXiv:1804.11326.
[58] M. Schuld and N. Killoran, Phys. Rev. Lett. **122**, 040504 (2019), arXiv:1803.07128 [quant-ph].
[59] Y. Liu, S. Arunachalam, and K. Temme, Nat. Phys. **17**, 1013 (2021), arXiv:2010.02174 [quant-ph].
[60] J. R. Glick, T. P. Gujarati, A. D. Corcoles, Y. Kim, A. Kandala, J. M. Gambetta, and K. Temme, Covariant quantum kernels for data with group structure (2021), arXiv:2105.03406 [quant-ph].
[61] X. Gao and L.-M. Duan, Nat Commun **8**, 662 (2017), arXiv:1701.05039 [cond-mat, physics:quant-ph].

Appendix A: Definitions

Definition 12 (density matrix)**.** pure state $|\psi\rangle$; A quantum state ρ is defined to be a positive operator $\rho \in \mathrm{End}(V)$ with $\mathrm{Tr}(\rho) = 1$. density matrix ρ (trace one, Hermitian, PSD)...

Definition 13 (POVM)**.** A positive-operator valued measurement (POVM) M consists of a set of positive operators that sum to the identity operator $\mathbb{1}$. When a measurement $M = \{E_1, \ldots, E_k\}$ is applied to a quantum state ρ, the outcome is $i \in [k]$ with probability $p_i = \mathrm{tr}(\rho E_i)$. observables ... $\mathbb{E}[x] \equiv \langle O_x \rangle := \mathrm{tr}(O_x \rho)$

Definition 14 (positive, semidefinite)**.** denoted $X \preceq Y$ provided $Y - X$ is positive

Definition 15 (partial trace)**.** reduced density matrix $\rho_A = \mathrm{Tr}_B(\rho_{AB})$

Remark 2. a pure (bipartite) state is entangled iff the reduced state $\rho^A = \mathrm{Tr}_A(\rho)$ is mixed. The mixedness of this reduced state allows one to quantify the amount of entanglement in this state.

Definition 16 (partial transpose)**.** [7] The partial transpose (PT) operation - acting on subsystem A - is defined as

$$|k_A, k_B\rangle\langle l_A, l_B|^{\intercal_A} := |l_A, k_B\rangle\langle k_A, l_B| \tag{A1}$$

where $\{|k_A, k_B\rangle\}$ is a product basis of the joint system AB.

Definition 17 (maximally entangled)**.** a state vector is *maximually entangled* iff the reduced state at one qubit is maximally mixed, i.e., $\mathrm{Tr}_A(|\psi\rangle\langle\psi|) = \frac{1}{2}$.

Definition 18 (Schmidt measure)**.** Consider the following bipartite pure state, written in Schmidt form:

$$|\psi\rangle = \sum_i^r \sqrt{\lambda_i}\, |\phi_i^A\rangle \otimes |\phi_i^B\rangle \tag{A2}$$

where $\{|\phi_i^A\rangle\}$ is a basis for $\mathcal{H}_A$ and $\{|\phi_i^A\rangle\}$ for $\mathcal{H}_B$. The strictly positive values $\sqrt{\lambda_i}$ in the Schmidt decomposition are its *Schmidt coefficients*. The number of Schmidt coefficients, counted with multiplicity, is called its *Schmidt rank*, or Schmidt number. (Schmidt rank ?? $\mathrm{SR}^A(\psi) = \mathrm{rank}(\rho_\psi^A)$) Schmidt measure is minimum of $\log_2 r$ where r is number of terms in an expansion of the state in product basis.

Definition 19 (entropy)**.** In quantum mechanics (information), the von Neumann *entropy* of a density matrix is $H_N(\rho) := -\mathrm{Tr}(\rho \log \rho) = -\sum_i \lambda_i \log(\lambda_i)$; In classical information (statistical) theory, the Shannon entropy of a probability distribution P is $H_S(P) := -\sum_i P(x_i) \log P(x_i)$. relative entropy (**??**)

Definition 20 (entanglement entropy)**.** The bipartite *von Neumann entanglement entropy* S is defined as the von Neumann entropy of either of its reduced density matrix ρ_A. For a pure state $\rho_{AB} = |\Psi\rangle\langle\Psi|_{AB}$, it is given by

$$E(\Psi_{AB}) = S(\rho_A) = -\mathrm{Tr}(\rho_A \log \rho_A) = -\mathrm{Tr}(\rho_B \log \rho_B) = S(\rho_B) \tag{A3}$$

where $\rho_A = \mathrm{Tr}_B(\rho_{AB})$ and $\rho_B = \mathrm{Tr}_A(\rho_{AB})$ are the reduced density matrices for each partition. With Schmidt decomposition (Eq. (A2)), the entropy of entanglement is simply $-\sum_i p_i^2 \log(p_i)$. the nth Renyi entropy, $S_n = \frac{1}{n-1}\log(R_n)$ where $R_n = \mathrm{Tr}(\rho_A^n)$

Example 1. The Schmidt measure for any multi-partite GHZ states is 1, because there are just two terms. Schmidt measure for 1D, 2D, 3D-cluster state is $\lfloor \frac{N}{2} \rfloor$. Schmidt measure of tree is the size of its minimal vertex cover[??].

Definition 21 (fidelity)**.** Given a pair of states (target ρ and prepared ρ'), Uhlmann fidelity $F(\rho,\rho') := \mathrm{Tr}\left(\sqrt{\sqrt{\rho}\rho'\sqrt{\rho}}\right) \equiv \left\|\sqrt{\rho}\sqrt{\rho'}\right\|_1$, where $\sqrt{\rho}$ dentoes the positive semidefinite square root of the operator ρ. (infidelity $1-F(\rho,\rho')$) For any mixed state ρ and pure state $|\psi\rangle$, $F(\rho,|\psi\rangle\langle\psi|) = \sqrt{\langle\psi|\rho|\psi\rangle} \equiv \sqrt{\mathrm{Tr}(\rho\,|\psi\rangle\langle\psi|)}$ which can be obtained by the Swap-test[?]. linear fidelity or overlap $F(\rho,\rho') := \mathrm{tr}(\rho\rho')$.

different distance measures [54]

Notation 4 (norm)**.** Schatten p-norm $\|x\|_p := (\sum_i |x_i|^p)^{1/p}$. Euclidean norm l_2 norm; Spectral (operator) norm $\|\mathbf{x}\|_\infty$; Trace norm $\|A\|_{\mathrm{Tr}} \equiv \|A\|_1 := \mathrm{Tr}(|A|) \equiv \mathrm{Tr}\left(\sqrt{A^\dagger A}\right)$, $|A| := \sqrt{A^\dagger A}$, $p=1$; Frobenius norm $\|A\|_F := \sqrt{\mathrm{Tr}(A^\dagger A)}$, $p=2$; Hilbert-Schmidt norm $\|A\|_{HS} := \sqrt{\sum_{i,j} A_{ij}^2} =? \sum_{i\in I} \|Ae_i\|_H^2$; Hilbert-Schmidt inner product $\langle A,B\rangle_{\mathrm{HS}} := \mathrm{Tr}\left(A^\dagger B\right)$, Frobenius inner product $\langle A,B\rangle_{\mathrm{F}} := \mathrm{Tr}\left(A^\dagger B\right)$? (in finite-dimensionala Euclidean space, the HS norm is identical to the Frobenius norm) Although the Hilbert-Schmidt distance is arguably not too meaningful, operationally, one can use Cauchy-Schwarz to relate it to the very natural trace distance. shadow norm ...

Definition 22 (distance)**.** For mixed states, trace distance $d_{\mathrm{tr}}(\rho,\rho') := \frac{1}{2}\|\rho-\rho'\|_1$. For pure states, $d_{\mathrm{tr}}(|\psi\rangle, |\psi'\rangle) := \frac{1}{2}\||\psi\rangle\langle\psi| - |\psi'\rangle\langle\psi'|\|_1 = \sqrt{1-|\langle\psi|\psi'\rangle|^2}$. fidelity and trace distance are related by the inequalities

$$1 - F \le D_{\mathrm{tr}}(\rho,\rho') \le \sqrt{1-F^2} \tag{A4}$$

variation distance of two distribution $d_{var}(p,p') := \frac{1}{2}\sum_i |p_i - p_i'| = \frac{1}{2}\|p-p'\|_1$. l_2 distance ... Hellinger distance ... HS distance $D_{\mathrm{HS}}(\rho,\rho') := \|\rho-\rho'\|_{\mathrm{HS}} = \sqrt{\mathrm{Tr}((\rho-\rho')^2)}$

denote a group by $\mathbb{G}$ and a subgroup $\mathbb{H}$.

Definition 23 (Pauli group)**.**

Definition 24 (Clifford group)**.**

Definition 25 (Stabilizer)**.** An observable S_k is a stabilizing operator of an n-qubit state $|\psi\rangle$ if the state $|\psi\rangle$ is an eigenstate of S_k with eigenvalue 1,
A stabilizer set $S = \{S_1,\ldots,S_n\}$ consisting of n mutually commuting and independent stabilizer operators is called the set of stabilizer "generators".

Many highly entangled n-qubit states can be uniquely defined by n stabilizing operators which are locally measurable, i.e., they are products of Pauli matrices. A stabilizer S_i is an n-fold tensor product of n operators chosen from the one qubit Pauli operators $\{\mathbb{1}, X, Y, Z\}$. An n-partite(qubit) graph state can also be uniquely determined by n independent stabilizers, $S_i := X_i \bigotimes_{j\in n} Z_j$, which commute with each other and $\forall i, S_i|G\rangle = |G\rangle$.?? The graph state is the unique eigenstate wtih eignevalue of $+1$ for all the n stabilizers. As a result, a graph state can be written as a product of stailizer projectors, $|G\rangle\langle G| = \prod_{i=1}^n \frac{S_i+\mathbb{1}}{2}$. Stabilizer formalism

Example 2 (GHZ)**.** For GHZ state: $|\mathrm{GHZ}\rangle := \frac{1}{\sqrt{2}}(|0\rangle^{\otimes n} + |1\rangle^{\otimes n})$, the projector based witness

$$W_{\mathrm{GHZ}_3} = \frac{1}{2}\mathbb{1} - |\mathrm{GHZ}\rangle\langle\mathrm{GHZ}| \tag{A5}$$

requires four measurement settings. For three-qubit GHZ state [23], the local measurement witness

$$W_{\mathrm{GHZ}_3} := \frac{3}{2}\mathbb{1} - X^{(1)}X^{(2)}X^{(3)} - \frac{1}{2}\left(Z^{(1)}Z^{(2)} + Z^{(2)}Z^{(3)} + Z^{(1)}Z^{(3)}\right) \tag{A6}$$

This witness requires the measurement of the $\left\{\hat\sigma_x^{(1)}, \hat\sigma_x^{(2)}, \hat\sigma_x^{(3)}\right\}$ and $\left\{\hat\sigma_z^{(1)}, \hat\sigma_z^{(2)}, \hat\sigma_z^{(3)}\right\}$ settings. For n-qubit case, detect genuine n-qubit entanglement close to GHZ_n

$$W_{\mathrm{GHZ}_n} = (n-1)\mathbb{1} - \sum_{k=1}^n S_k(\mathrm{GHZ}_n) \tag{A7}$$

where $\hat S_k$ is the Stabilizer ... [5] Detecting Genuine Multipartite Entanglement with Two Local Measurements [23]

graph state is an important large class of multipartite states in quantum information, because (connected) graph states represent a large class of genuine multipartite entangled states that have concise representations. Typical graph states include cluster states, GHZ states, and the states involved in error correction (toric code). It worth noting that 2D cluster (rectangular lattice graph) state is the universal resource for the measurement based quantum computation (MBQC) [2].

Definition 26 (cluster state)**.** 1D four qubits

$$\left|\psi_4^{1D}\right\rangle = \frac{1}{2}(|+00+\rangle + |+01-\rangle + |-10+\rangle - |-11-\rangle) \tag{A8}$$

The entanglement in a graph state is related to the topology of its underlying graph [55].

Remark 3. LU, LC equivalence, local operations and classical communication (LOCC),

Definition 27 (graph state)**.** Given a simple graph (undirected, unweighted, no loop and multiple edge) $G = (V, E)$, a graph state is constructed as from the initial state $|+\rangle^{\otimes n}$ corresponding to n vertices. Then, apply controlled-Z gate to every edge, that is $|G\rangle := \prod_{(i,j)\in E} \mathsf{cZ}_{(i,j)} |+\rangle^{\otimes n}$ with $|+\rangle := (|0\rangle + |1\rangle)/\sqrt{2}$.

Question 1. *how to relate graph state entanglement to graph property test ..??. (graph kernel??) [55]. witness; bounds;* **??***? vertex cover? Hamiltonian cycle of a graph state?*

	$\|\text{GHZ}_3\rangle$	$\|W_3\rangle$	$\|CL_3\rangle$	$\|\psi_2\rangle$	$\|\mathcal{D}_{2,4}\rangle$	$\|\text{GHZ}_n\rangle$	$\|W_3\rangle$	$\|G_n\rangle$
α	1/2	2/3	1/2	3/4	2/3	1/2	$(n-1)/n$	1/2
maximal p_{noise}	4/7	8/21	8/15	4/15	16/45	$1/2 \cdot (1-1/2^n)^{-1}$		
local measurements	4	5	9	15	21	$n+1$	$2n-1$	depend on graphs

TABLE III: [21]

Appendix B: Machine learning background

Notations: The (classical) training data (for supervised learning) is a set of m data points $\left\{(\mathbf{x}^{(i)}, y^{(i)})\right\}_{i=1}^m$ where each data point is a pair $(\mathbf{x}, y)$. Normally, the input (e.g., an image) $\mathbf{x} := (x_1, x_2, \ldots, x_d) \in \mathbb{R}^d$ is a vector where d is the number of *features* and its *label* $y \in \Sigma$ is a scalar with some discrete set Σ of alphabet/categories. For simplicity and the purpose of this paper, we assume $\Sigma = \{-1, 1\}$ (binary classification).

1. Support vector machine

SVM is a typical supervised learning algorithm for classification. Taking the example of classifying cat/dog images, supervised learning means we are given a dataset in which every image is labeled either a cat or a dog such that we can find a function classifying new images with high accuracy. More precisely, the training dataset is a set of pairs of features X and their labels y. In the image classification case, features are obtained by transforming all pixels of an image into a vector. In SVM, we want to find a linear function, that is a hyperplane which separates cat data from dog data. So, the prediction label is given by the sign of the inner product (projection) of the hyperplane and the feature vector. We can observe that the problem setting of image classification by SVM is quite analogous to entanglement detection, where input data are quantum states now and the labels are either entangled or separable.

Definition 28 (SVM)**.** Given a set of (binary) labeled data, support vector machine (SVM) is designed to find a hyperplane (a linear function) such that maximize the margin between two partitions...

$$\max_{\mathbf{w}} \|\mathbf{w}\|^2 \text{ s.t. } \forall i, y^{(i)} \cdot (\mathbf{w} \cdot \mathbf{x} + b) \geq 1. \tag{B1}$$

Lagrange multipliers α

$$L = \frac{1}{2}\|\mathbf{w}\|^2 - \sum_i^m \alpha^{(i)} \left(\mathbf{w} \cdot \mathbf{x}^{(i)} + b\right) + \sum_i^m \alpha^{(i)} \tag{B2}$$

a. kernel method

However, note that SVM is only a linear classifier. while most real-world data, such as cat/dog images and entangled/separable quantum states are not linearly separable. For example, with this two dimension dataset, we are unable to find a hyperplane to separate red points from the purple points very well. Fortunately, there is a very useful tool called kernel method or kernel trick to remedy this drawback. The main idea is mapping the features to a higher dimensional space such that they can be linearly separated in the high dimensional feature space. Just like this example, two dimensional data are mapped to the three dimensional space. Now, we can easily find the separating plane. With SVM and kernel methods, we expect to find a generic and flexible way for entanglement detection. kernel

Definition 29 (kernel)**.** In general, the kernel function $k : \mathcal{X} \times \mathcal{X} \to \mathbb{R}$ measures the similarity between two input data points by an inner product

$$k(\mathbf{x}, \mathbf{x}') := \langle \phi(\mathbf{x}), \phi(\mathbf{x}') \rangle \tag{B3}$$

If the input $\mathbf{x} \in \mathbb{R}^d$ (conventional machine learning task, e.g., image classification), the feature map $\phi(\mathbf{x}) : \mathbb{R}^d \to \mathbb{R}^n$ $(d < n)$ from a low dimensional space to a higher dimensional space. The corresponding kernel (Gram) matrix $\mathbf{K}$ should be a positive, semidefinite (PSD) matrix, i.e. all eigenvalues are non-negative

Example 3 (kernels)**.** Some common kernels: the polynomial kernel $k_{\text{poly}}(\mathbf{x}, \mathbf{x}') := (1 + \mathbf{x} \cdot \mathbf{x}')^q$ with feature map $\phi(\mathbf{x})$ ... The Gaussian kernel $k_{\text{gaus}}(\mathbf{x}, \mathbf{x}') := \exp\left(-\gamma \|\mathbf{x} - \mathbf{x}'\|_2^2\right)$ with an infinite dimensional feature map $\phi(\mathbf{x})$. An important feature of kernel method is that kernels can be computed efficiently without evaluating feature map (might be infinite dimension) explicitly.

Definition 30 (graph kernel)**.** given a pair of graphs (G, G'), *graph kernel* is $k(G, G') =$. quantum graph kernel $k(G, G') = |\langle G|G' \rangle|^2$?? [56]

b. Quantum kernel

related works:

- quantum kernel method: estimate kernels by quantum algorithms (circuits) [57] [58]: for classical problem (data)
- rigorous and robust quantum advantage of quantum kernel method in SVM [59]. group structured data [60]
- power of data in quantum machine learning [47]: input??? projected quantum kernel

Definition 31 (quantum kernel)**.** quantum kernel with quantum feature map $\phi(\mathbf{x}) : \mathcal{X} \to |\phi(\mathbf{x})\rangle\langle\phi(\mathbf{x})|$

$$k_Q(\rho, \rho') := |\langle \phi(\mathbf{x}) | \phi(\mathbf{x}') \rangle|^2 = \left| \langle 0 | U_{\phi(\mathbf{x})}^\dagger U_{\phi(\mathbf{x}')} | 0 \rangle \right|^2 =? \operatorname{Tr}(\rho\rho') \equiv \langle \rho, \rho' \rangle_{\text{HS}} \tag{B4}$$

where $U_{\phi(\mathbf{x})}$ is a quantum circuit or physics process that encoding an input $\mathbf{x}$. In quantum physics, quantum kernel is also known as transition amplitude (quantum propagator);

c. neural network and kernel

Definition 32 (neural tagent kernel)**.** neural tangent kernel [39]: proved to be equivalent to deep neural network [61] in the limit ...

$$k_{\text{NT}}\left(S_T(\rho_l), \tilde{S}_T(\rho_{l'})\right) = \left\langle \phi^{(\text{NT})}(S_T(\rho_l)), \phi^{(\text{NT})}(\tilde{S}_T(\rho_l)) \right\rangle \tag{B5}$$